

1 Breakthrough Technologies

2

3 Optical Measurement of Stem Xylem Vulnerability

4 Timothy J. Brodribb, Marc Carriqui, Sylvain Delzon and Christopher Lucani

5 **Abstract:** The vulnerability of plant water transport tissues to a loss of function by cavitation during
6 water stress is a key indicator of the survival capabilities of plant species during drought. Quantifying
7 this important metric has been greatly advanced by non-invasive techniques that allow embolisms to
8 be directly viewed in the vascular system. Here we present a new method for evaluating the spatial
9 and temporal propagation of embolising bubbles in the stem xylem during imposed water stress. We
10 demonstrate how the “optical method”, previously used in leaves, can be adapted to measure the
11 xylem vulnerability of stems. Validation of the technique is carried out by measuring the xylem
12 vulnerability of 13 conifers and two short vesselled angiosperms and comparing results with
13 measurements made using the “cavitron” centrifuge method. Very close agreement between the
14 two methods confirms the reliability of the new optical technique, and opens the way to simple,
15 efficient and reliable assessment of stem vulnerability using standard flatbed scanners, cameras or
16 microscopes.

17

18 INTRODUCTION

19 In modern tracheophytes xylem cavitation constitutes a fundamental limitation to the functionality
20 of water transport systems. As a consequence, the ability of species to resist or avoid cavitation
21 forms a primary axis of adaptation and ecological variation among land plants (Xu et al., 2016).
22 However, despite the tremendous ecological and physiological insights that await a detailed
23 understanding of the limits and spread of xylem cavitation in plant species, rapid progress has been
24 limited by technical difficulties. These difficulties are largely associated with replicating, under
25 experimental conditions, the metastable hydraulic environment that characterizes water flowing in
26 the xylem when exposed to the large tensions that exist during rapid transpiration or soil water
27 deficit (Cochard et al., 2013).

28 Most traditional methods of quantifying the degree of xylem embolism require excision of plant
29 parts (stems, roots or leaves), causing air or exogenous water to be rapidly sucked into the
30 vasculature, thereby substantially perturbing the vascular system prior to measurement (Ennajeh et
31 al., 2011; Rockwell et al., 2014). A substantial advance in recent years has been the use of imaging
32 technology that allows water to be viewed inside intact plants, revealing the location and formation
33 of embolisms inside stems (Broderson et al., 2013), roots (Cuneo et al., 2016), leaves (Bouche et al.,
34 2015; Brodribb et al., 2016; Scoffoni et al., 2017), and flowers (Zhang and Brodribb, 2017). These
35 studies have substantially changed our view of xylem cavitation and repair, indicating that cavitation
36 can propagate quickly between plant organs (Skelton et al., 2017), and that air blockages (embolisms)
37 are not rapidly repaired in trees after re-watering (Choat et al., 2015; Charrier et al., 2016).
38 Cavitation is now widely viewed as a long-term damage to the water transport system of trees, that

39 occurs under significant water stress, and that is repaired by regrowth of new xylem tissue (Brodribb
40 et al., 2010; Cochard and Delzon, 2013).

41 Imaging with x-ray provides unrivalled spatial information about where cavitation occurs in stems
42 and can be used to determine the vulnerability of xylem to cavitation in plant species (Choat et al.,
43 2015; Nolf et al., 2017). However the damaging nature of the x-ray beam means that high frequency
44 imaging during the hours and days required to dehydrate plants to water stresses sufficient to cause
45 cavitation is not possible. Magnetic resonance imaging on the other hand can provide spatial and
46 temporal information about cavitation, but low image resolution (pixel sizes larger than the vessels
47 of most species) means that MRI can only be used to resolve embolisms in species with very large
48 vessels. Both techniques require large and expensive hardware and are not currently usable in the
49 field, thus having limited application for measuring large sample sizes. An alternative to these
50 hardware-intensive methods was recently developed using an optical technique measures changes
51 in visual light transmission caused by cavitation in leaf veins (Brodribb et al., 2016). This technique
52 was developed following observations of cavitation bubbles in excised conifer tracheids
53 (Ponomarenko et al., 2014), and provides detailed information about the spatial and temporal
54 evolution of cavitation in the venation network of leaves exposed to water stress. The calculated
55 “vulnerability” of leaf xylem to cavitation (expressed as a P_{50} , or potential required to deactivate 50%
56 of xylem function) using this Optical Vulnerability (OV) method agrees closely with hydraulically
57 measured P_{50} in leaves (Brodribb et al., 2016), indicating the utility of the method for quantifying
58 hydraulic failure . Importantly, the OV method requires only a flatbed scanner or camera to collect
59 vulnerability information, thus providing a cost effective and portable means of assessing leaf xylem
60 vulnerability.

61 Although the OV method has a demonstrated capacity to reveal leaf vulnerability to water stress,
62 one of the primary applications of xylem cavitation physiology is in the prediction of tree mortality
63 (Anderegg et al., 2015) and species distribution (Larter et al.), and in these applications stem
64 vulnerability may provide a more definitive mortality threshold than leaves. Studies of potted plants
65 have shown that failure of the stem xylem corresponds closely to the point of tree mortality during
66 acute drought stress (Brodribb and Cochard, 2009; Urli et al., 2013), as might be expected
67 considering the fact that embolism of the stem effectively isolates the leaves from soil water. A
68 vulnerability gradient from stems to leaves is evident in some species (Tyree et al., 1993) (but
69 probably not in herbs (Skelton et al., 2017)), and is hypothesized to be a way that woody plants
70 protect their more energy expensive stem investment by sacrificing leaves during extreme drought
71 (Zimmermann, 1983; Hochberg et al., 2017). Given the importance of understanding stem
72 vulnerability in woody plants we sought here to extend the highly efficient OV method in leaves, to
73 stems. We postulated that the same principle used to identify cavitation in leaves, recording changes
74 in light transmission caused by a transition from liquid to air filled xylem conduits during cavitation,
75 could be used in stems. Indeed it has been known for a long time that air bubbles can be visualized
76 in stems by light microscopy (Vesque, 1883), and the same principle was used 80 years ago as a way
77 of identifying the presence of water or air in branches by the evolution of light coloured streaks in
78 the wood after it had been pricked with a sharp scalpel (Haines, 1935). Here we utilize the principal
79 that a transition from a water-containing, to an air-filled conduit during cavitation will cause a
80 distinct colour change in visible conduits from translucent (typically dark) to reflective (white) tissue.
81 Thus we quantify spatially discrete changes in the refractive index of the stem. Continuous

82 observation of drying stems should thus allow the timing and pattern of cavitation to be recorded
83 and quantified in relation to concurrent measurements of stem water potential.

84 In order to cross-validate the new stem optical method here we use a traditional hydraulic
85 centrifuge method as a standard reference for comparison. The centrifuge method has long been
86 considered an accurate method for assessing xylem vulnerability, except in cases where maximum
87 vessel lengths are similar to the diameter of the centrifuge rotor (Cochard et al., 2013). For this
88 reason we focussed on a diverse group of conifers which lack long xylem conduits, and two short
89 vessel angiosperms were also included to maximize the breadth of the species sample.

90

91 RESULTS

92 Cavitation was easily resolved visually, and could be readily quantified by applying image difference
93 to distinguish fast changes in light reflection due to xylem cavitation from slow movements
94 associated with branch deformation during drying. The onset of cavitation was recorded on average
95 1308 minutes after branch excision, but ranged from 420 to 2230 minutes. In all species, the
96 cumulative total of cavitations recorded followed an approximately sigmoidal function, although this
97 was never a completely smooth function, typically being punctuated by blocks of major cavitation
98 (Fig.1, Fig. 2). These blocks of cavitation often involved hundreds of tracheids in the conifers, and
99 typically became larger as water potential approached P_{50} , before diminishing in size towards the end
100 of the drying process. Typically, many cavitation events were recorded in the same part of the stem
101 due to the multiple layers of overlaying xylem that were represented in the 2D image differences.
102 The total cavitated area was typically 150-200% of the 2D area of the exposed stem (due to multiple
103 layers of conduits).

104 Cavitation in the two species of angiosperms also appeared to involve groups of conduits,
105 particularly during the period of maximum intensity of cavitation around P_{50} (Fig. 2). But smaller
106 events, presumably representing individual conduits, were often observed as early events, or as a
107 tail towards the end of the cavitation process (Fig. 2).

108 Large differences in P_{50} were recorded between species using the optical method, with means
109 ranging from -1.2MPa in *Retrophyllum comptonii* to -9.1MPa in *Diselmia archeri*. Within species
110 variation was also significant in many species, reaching a maximum in *Diselmia archeri* where P_{50}
111 ranged between -6.7 and -11.2 MPa between individuals. On average the coefficient of variation in
112 P_{50} among replicate branches was 16.2% using the optical method and 9.2% using the cavitron.
113 Mean slopes of the vulnerability curves for each species (between 12% and 88% loss of function)
114 were correlated between the two methods, but the optical method produced steeper slopes on
115 average.

116 Among the conifer species there was strong agreement between P_{50} determined with the optical
117 technique and centrifuge techniques. A regression slope of 0.997 ($r^2=0.93$) was found between
118 optical and centrifuge P_{50} in the 12 conifer species, and the ranking of P_{50} was very similar using both
119 methods.

120 One of the two angiosperms sampled showed a significant difference between the optical and
121 centrifuge P_{50} . Although both techniques found *Rosmarinus* samples to be highly cavitation resistant,
122 P_{50} on the centrifuge (-12MPa) was 32% more negative than the optical method (-8.1MPa).

123

124 DISCUSSION

125 A new optical method for visualizing the process of xylem cavitation in plants is shown here to
126 quantify the vulnerability of stem xylem to cavitation-induced reductions in hydraulic function of the
127 stem xylem. The process of cavitation damage to the stem vascular system during water stress could
128 be tracked in time and space on the stems of a diversity of species including woody conifers and
129 angiosperms. This novel technique represents a very easy and cheap new method for assessing stem
130 vulnerability in woody species using excised branches. In principle, the method can also be used on
131 attached branches, although this was not tested here.

132 The optical technique allows direct visualization of the process of cavitation in stems under realistic
133 conditions of plant desiccation (as opposed to centrifugation or stem pressurization). Apart from its
134 simplicity, the advantage of this technique is that it provides a complete view of the spatial and
135 temporal progression of cavitation in stems during increasing water stress. This new perspective of
136 stem cavitation means that continuous monitoring of stem cavitation is possible as bubbles
137 propagate axially in the stem during the development of increasing water deficit. Although cross-
138 validation of the technique was performed using woody stems, the technique also works well in
139 herbaceous species, where more translucent stems often do not require phloem removal.

140 The precisely resolved temporal dynamics of stem cavitation in both conifers and angiosperms
141 studied here all yielded vulnerability curves that were highly sigmoidal in shape, characterized by an
142 initial, extended period of stem desiccation before any stem cavitation events were recorded. This
143 sigmoidal form of xylem vulnerability measured by the OV technique closely matches the form of
144 cavitron (Lamy et al., 2011) and x-ray CT (Choat et al., 2015) vulnerability curves. The majority of
145 data collected using traditional bench drying methods of measuring xylem vulnerability also produce
146 sigmoidal vulnerability curves, but more linear curves are often reported in species with highly
147 stress-resistant xylem (Markesteyn et al., 2011; Vinya et al., 2013). One important benefit of the OV
148 and CT methods of assessing vulnerability is that they report the responses of functioning xylem
149 without reference to a “flushed” condition. The flushing procedure is required by other hydraulic
150 techniques, whereby samples are subjected to high water pressure to fill all airspaces in the sample
151 and provide a theoretical maximum conductance. Flushing has the potential to activate (refill) xylem
152 that was non-functional xylem in the intact plant, as well as introducing bubble nuclei, both of which
153 can produce erroneous vulnerability curves (Rockwell et al., 2014).

154 Among the range of alternative methods for measuring xylem vulnerability, the cavitron was
155 selected here as a standard for comparison because it is considered to be highly reliable when used
156 to measure species with short conduits such as conifers (Cochard et al., 2013). For this reason most
157 of our sample set was taken from the conifer clade, using the same individuals for both optical
158 (sampled in 2016) and cavitron (sampled in 2012) techniques. The accuracy of centrifuges for
159 measuring angiosperm xylem vulnerability is the subject of considerable debate due to probable
160 artefacts associated with long vessels (Torres - Ruiz et al., 2014; Hacke et al., 2015). For this reason

161 we only measured two species of angiosperms, selected to cover a range of sensitivity to water
162 stress, but both of which had maximum xylem vessel lengths that were approximately half that of
163 the rotor diameter. Despite the huge difference in vulnerability between the two angiosperms
164 measured here, both were found to produce a sigmoidal form in their vulnerability curves using both
165 optical and cavitron methods. Our predawn sampling of well watered trees ensured that sampled
166 branches started drying from water potentials close to zero, thus ensuring a minimum of native
167 embolism in the measured samples.

168 The optical method assesses the loss in xylem function in terms of a cumulative area of stem
169 cavitated in each frame of image sequences. This area-based calculation does not account for the
170 profound influence of xylem conduit radius, in the order of r^4 , that should determine the flow
171 penalty incurred by cavitation of any particular conduit in the stem (Sperry et al., 2006). Despite this
172 apparent limitation there was very strong agreement in P_{50} between the optical method (reporting
173 area of cavitated conduits) and the centrifuge method (quantifying losses in hydraulic conductance).
174 The explanation for the strong agreement between techniques despite different metrics of
175 cavitation is clearly evident from the spatiotemporal distribution of cavitation in stems observed
176 here. Most significant is the evolution of cavitation in large blocks of connected conduits as opposed
177 to discrete conduits, particularly as stems approached the P_{50} water potential. These large
178 interconnected cavitation events are also seen in x-ray images of stems (Choat et al., 2015b), and
179 produce a steep slope in the vulnerability curve around P_{50} . Assuming that cavitation in stems on the
180 centrifuge also proceeds in this fashion, then it would be expected that P_{50} s produced by the two
181 techniques would agree. The optical technique emphasizes the importance of connections between
182 conduits more than the size of individual vessels, and due to the nature of cavitation propagation,
183 this is likely to accurately capture the dynamics of flow restriction. Although the slopes of
184 vulnerability curves produced by the cavitron tended to be shallower than those using the optical
185 method, this may be explained by the smaller diameter branches used on the optical versus
186 cavitron technique. Small (3-6mm) diameter branches were used for the optical measurements to
187 ensure cavitations could be visualized from all depths in the stem. Larger diameter stem samples
188 used in the cavitron measurements are likely to incorporate more than one year of growth in the
189 sampled branch, particularly considering the slow growth of many of the conifer species used here
190 for comparison. Thus the cavitron curves reflect the integrated vulnerability of a much larger sample
191 of tracheids than the < one year old stems measured by the optical method, likely leading to a
192 shallower slope (Torres Ruiz et al., 2016).

193 A significant discrepancy between P_{50} in optical and centrifuge methods was only observed in stems
194 of the angiosperm *Rosmarinus*. Although both methods recorded extremely high cavitation
195 resistance in this species, the cavitron produced a more negative P_{50} . Further examination of this
196 species and other highly resistant angiosperms will be needed to determine whether this
197 disagreement is due to artefacts or some systematic bias of one of the two methods. One possible
198 contributing factor is the long travel time from Hobart to France prior to measurement of this
199 individual. Samples of the same species measured locally with the cavitron yielded values much
200 closer to the OV value (Herve Cochard, *pers. comm*). This very resistant end of the vulnerability
201 spectrum is of particular interest as it appears as a critical adaptation in both conifer (Larter et al.;
202 Brodribb et al., 2014) and angiosperm (Blackman et al., 2012) tree species inhabiting semi-arid
203 woodland.

204 The success of the optical method in providing a time resolved map of cavitation in water stressed
205 stems, while yielding an accurate measure of vulnerability in terms of P_{50} , opens the door to new
206 applications. The simplicity and low cost of the technique makes it highly appealing for ecological
207 and genetic research where large sample sizes are required. In addition the technique provides a
208 means of viewing cavitation in tissues that have been difficult to measure. Flowers have recently
209 been successfully measured using the optical method to show embolism relative to leaves in herbs
210 and woody species (Zhang and Brodribb, 2017), while roots present an obvious future target. The
211 optical method is ideally suited to explore how cavitation moves within and between plant tissues as
212 water stress intensifies, and has the potential to provide an integrated view of cavitation in major
213 plant organs as cavitation propagates within an individual.

214

215 MATERIALS AND METHODS

216 *Plant Material*

217 Thirteen species of conifers from four conifer families (Table I) were sampled from a potted conifer
218 collection growing in glasshouses at the University of Tasmania. All plants were >10 years old and
219 were growing in 20L pots under well watered conditions in partially open glasshouses such that light
220 and temperature were close to ambient conditions in Hobart (Australia). Samples for centrifuge
221 analysis were collected and measured in 2012 while samples for optical analysis were made in 2016
222 on the same individuals or clones. All species were represented by three replicates collected as
223 cuttings from different individuals in the wild, or wild collected seeds. In addition we collected two
224 angiosperms with contrasting water stress tolerance to represent opposite ends of the angiosperm
225 vulnerability spectrum, but which had relatively short vessels such that they could be measured
226 using the centrifuge technique. These two species (*Rosmarinus officinalis* and *Betula pendula*) were
227 both collected at the end of a wet spring (2016) from single garden plants in Hobart.

228 *Cavitron stem vulnerability*

229 We carried out measurements on one or two branches from three to 16 trees per species.
230 Transpiration losses were prevented by removing the needles or leaves immediately after sampling
231 and wrapping the branches in moist paper to keep them humid and cool (5°C) until the
232 measurement of embolism resistance (within three weeks of sampling). All samples were sent via an
233 international express shipping company to France within three days. Vulnerability to drought-
234 induced embolism was then determined at the Caviplace (University of Bordeaux, Talence, France;
235 <http://sylvain-delzon.com/caviplace>) with the Cavitron technique (Cochard, 2002; Cochard et al.,
236 2005). The bark was removed from conifer branches before sampling, to prevent resin
237 contamination, and all branches were recut with a razor blade, under water, to a standard length of
238 0.27 m. The percentage loss of conductance (PLC) was determined at different speeds (i.e. different
239 xylem pressures) to obtain a vulnerability curve for each sample. These vulnerability curves show the
240 percentage loss of xylem conductance as a function of xylem pressure (see (Delzon et al., 2010) for
241 details). For each branch, the relationship between PLC and xylem water pressure was fitted with
242 the following sigmoidal equation (Pammenter and Van der Willigen, 1998):

$$PLC = \frac{100}{\left(1 + \exp\left(\frac{S}{25(P_i - P_{50})}\right)\right)}$$

243 where P_{50} (MPa) is the xylem pressure inducing a 50% loss of conductivity and S (% MPa⁻¹) is the
 244 slope of the vulnerability curve at the inflection point. Mean values of embolism vulnerability
 245 parameters (P_{50} and S) correspond to the average values of three to 16 samples per species.
 246 Additionally, we used our VCs to calculate P12 and P88, which are respectively the 12% and 88% loss
 247 of hydraulic conductivity. P12 and P88 are physiologically significant indexes because they are
 248 thought to respectively reflect the initial air-entry tension producing embolisms and the irreversible
 249 death-inducing xylem tension (Urli et al., 2013).

250 *Optical stem vulnerability*

251 The same individuals or clones of trees collected in 2012 for cavitron determination of P_{50} were
 252 revisited and sampled using the optical vulnerability method. Branches in the order of 1m long were
 253 cut from trees early in the morning and transferred in plastic bags to the laboratory about 50m away.
 254 Branches were generally allowed to equilibrate in moist plastic bags in the dark for a period of 60
 255 minutes to ensure stomata were closed before preparing the stem for imaging. The optical method
 256 cannot quantify existing embolism in the wood and is only able to measure new cavitations. For this
 257 reason great care was taken to ensure that samples were not exposed to any form of water stress or
 258 freezing in the months before measurement.

259 A stem psychrometer (ICT Australia) was fitted as close as possible to the region of stem being
 260 scanned for embolism formation. In fitting the psychrometer a small square of bark was removed
 261 avoiding damage to the wood. The psychrometer was partially insulated with polystyrene and set to
 262 log leaf water potential every 10 minutes. The cooling time for the psychrometer was increased from
 263 5s to 30s as stems dried, ensuring a stable reading of the wet-bulb temperature. Reference leaf
 264 water potentials were taken during the drying period using a Scholander pressure chamber, to
 265 ensure that leaf and stem water potentials were equilibrated, as would be expected due to stomatal
 266 closure prior to the commencement of cavitation (Brodribb and Holbrook, 2003). However, after
 267 stem cavitation had begun Scholander and psychrometer values often tended to diverge as would be
 268 expected due to hydraulic disconnection between leaves and stems.

269 A stem approximately 3-6mm in diameter and approximately 80-120 cm in length for conifers or 1-
 270 2m in length for the angiosperms, was selected for scanning. Branches that were actively elongating
 271 or expanding leaves were avoided to be sure that the xylem was mature (non-living). The depth of
 272 xylem that could be reliably visualized for cavitation was approximately 1mm, so a selection of stems
 273 were sectioned before-hand to determine the approximate branch thickness that would yield 1mm
 274 of xylem above the pith. A leafless region of the stem, approximately 15mm in length was prepared
 275 so that xylem on one side of the pith could be imaged. A region of bark approximately 15-20mm in
 276 length was carefully removed from one side of the stem to expose the underlying wood without
 277 causing damage the xylem. The easiest way of doing this was to run two parallel axial cuts along the
 278 bark either side of the desired window, avoiding damage to the underlying xylem, and to use a
 279 needle or fingernails to peel the bark gently back from the cuts. Once a window was created, it was
 280 firmly secured either onto a flatbed scanner (Perfection 800, Epson) or a microscope stage (Leica
 281 M205) using padded clamps to ensure no movement of the sample during drying. Once secured, the

282 scanner or camera was set to capture images at a rate of one per minute, and the sample left to dry
283 slowly until cavitations were no longer recorded (typically in the order of 48-120 hours). During
284 drying, the target region of the stem was mostly darkened except for the light of the microscope (a
285 ring illumination using LED lighting) or scanner. The rest of the stem was exposed to laboratory
286 lighting, and ambient conditions of 22°C and 55% RH. In the case of the scanner, images were
287 collected in normal reflective mode rather than the transmission mode used for leaves. Samples
288 were allowed to dry until no further cavitations could be seen in the xylem for a period of 12 hours.
289 In some samples, a thin layer of hydrogel (Tensive Gel, Parker USA) was applied to the exposed
290 xylem surface to improve light transmission and reduce evaporation from the surface. This had no
291 appreciable effect on the value of P_{50} when compared between samples (unpublished data) but care
292 was necessary to avoid reflections of movements as the gel shrinks during the drying process.

293 Once completed, image sequences were analysed to identify cavitation, which was easily seen as
294 changes in the reflection of the exposed xylem. Analysis by image difference using ImageJ (NIH), was
295 carried out by subtracting successive images to reveal fast changes in contrast produced by
296 cavitation. These rapid changes were easily identified in image subtractions, and could be filtered
297 from slow movements caused by drying. Thresholding of image differences allowed automated
298 counting of cavitation events using the “analyze stack” function in ImageJ. Full details including an
299 overview of the technique, image processing as well as scripts to guide image capture and analysis
300 are available at <http://www.opensourceov.org>.

301 A time-resolved count of cavitations in each stem, quantified as a number of pixels per event during
302 stem drying was compiled and this was converted to a % of total pixels cavitated. The psychrometer
303 output was then used to determine a fitted function that described the change in stem water
304 potential over time. Typically this was a linear function once stomata were closed, but occasionally
305 polynomial functions were fitted to account for variation in the slope $d\psi_{stem}/dt$. Combining the
306 cavitation count with the function describing $d\psi_{stem}/dt$ allowed the cumulative number of
307 cavitations to be expressed as a function of ψ_{stem} . The P_{50} for each sample stem was taken directly
308 from this plot. One value of P_{50} was measured for each of three stems, allowing a mean and SD to be
309 presented for each species.

310 ACKNOWLEDGEMENTS

311 Authors wish to thanks the Australian Research Council for funding to TB, and for a Postgraduate
312 Award to CL. MC received a travel grant from “La Caixa” Banking Foundation and from the
313 Conselleria d’Educació, Cultura i Universitats (Govern de les Illes Balears) and European Social Fund,
314 predoctoral fellowship FPI/1700/2014.

315

316

317 Table I- Species list

Species	Family	Class
<i>Agathis robusta</i> (C.Moore ex F.Muell.) F.M.Bailey	Araucariaceae	Conifer
<i>Araucaria bidwillii</i> Hook.	Araucariaceae	Conifer
<i>Araucaria cunninghamii</i> Mudie.	Araucariaceae	Conifer
<i>Wollemia nobilis</i> W.G.Jones, K.D.Hill & J.M.Allen	Araucariaceae	Conifer
<i>Callitris rhomboidea</i> R.Br. ex Rich. & A.Rich.	Cupressaceae	Conifer
<i>Diselma archeri</i> Hook.f.	Cupressaceae	Conifer
<i>Acmopyle pancheri</i> (Brongn. & Gris) Pilg.	Podocarpaceae	Conifer
<i>Afrocarpus falcatus</i> (Thunb.) C.N.Page	Podocarpaceae	Conifer
<i>Dacrycarpus imbricatus</i> (Blume) de Laub.	Podocarpaceae	Conifer
<i>Lagarostrobos franklinii</i> (Hook.f.) Quinn	Podocarpaceae	Conifer
<i>Phyllocladus aspleniifolius</i> (Labill.) Hook.f.	Podocarpaceae	Conifer
<i>Prumnopitys ladei</i> (F.M.Bailey) de Laub.	Podocarpaceae	Conifer
<i>Retrophyllum comptonii</i> (J.Buchholz) C.N.Page	Podocarpaceae	Conifer
<i>Retrophyllum rospigliosii</i> (Pilg.) C.N.Page	Podocarpaceae	Conifer
<i>Betula pendula</i> Roth	Betulaceae	Angiosperm
<i>Rosmarinus officinalis</i> L.	Lamiaceae	Angiosperm

318

319 .

320

321

322 FIGURE CAPTIONS

323 Figure 1. A- Cumulative area of cavitated xylem in a sample stem of *Callitris rhomboidea* is shown to
324 increase rapidly approximately 1 day after a hydrated branch was excised (time zero) and allowed to
325 dry. After a rapid rise in cavitation the rate of new xylem cavitated (quantified as number of pixels)
326 falls back to zero approximately 3 days after excision. The insert graph shows that the size of newly
327 cavitated regions visualized in the stem reaches a maximum during the steepest part of the curve
328 (insert). During this period, very large blocks of tracheids were cavitating in the 2 minute interval
329 between scans. B- Cumulative area of cavitated xylem expressed as a function of stem water
330 potential showing a classic sigmoidal vulnerability curve. C- A mosaic of colour maps showing the
331 spatial progression of cavitation through time in this 20mm long branched sample, the same stem
332 sample as B and C. Sequential blocks of 280 images have been stacked together (frame numbers
333 shown at the lower portion of each tile), with cavitated pixels coloured according to the water
334 potential at which cavitation occurred. In this sample the smaller branches proved to be more
335 resistant to cavitation than the main branch.

336 Figure 2. Similar plots as in Fig.1 showing the progression of cavitation in a stem of the angiosperm
337 *Rosmarinus officinalis*. Despite the extreme resistance to cavitation in this stem the vulnerability
338 curve shows a very steep transition from 12 to 88% cavitation. The reason for this steep transition
339 can be clearly seen as due to a number of large and long cavitations between frames 279 and 333.

340 Figure 3. A comparison of vulnerability curve shape produced by the cavitron (black circles) and the
341 optical method using branches from the same three individuals of the conifer *Lagarostrobos*
342 *franklinii*. Although the mean P_{50} is very similar in both species, the slope of the curves between 12%
343 and 88% were steeper using the optical method.

344 Figure 4. Mean P_{50} (\pm sd) for stems of the same individuals measured with the optical and cavitron
345 methods. Very close agreement was found in the conifer sample between methods (regression slope
346 0.98; $r^2= 0.93$). Among the two angiosperms sampled, good agreement was found in one species,
347 while the cavitron method produced a more negative P_{50} in the second. Slopes produced by the two
348 techniques (insert graph) were correlated ($r^2=0.35$; $p<0.05$), but the optical technique produced a
349 steeper slope in 14/16 species (1:1 shown as dotted line in each plot).

350

351 LITERATURE CITED

- 352 **Anderegg WRL, Flint A, Huang C-y, Flint L, Berry JA, Davis FW, Sperry JS, Field CB** (2015) Tree
 353 mortality predicted from drought-induced vascular damage. *Nature Geosci* **8**: 367-371
- 354 **Blackman CJ, Brodrribb TJ, Jordan GJ** (2012) Leaf hydraulic vulnerability influences species'
 355 bioclimatic limits in a diverse group of woody angiosperms. *Oecologia* **168**: 1-10
- 356 **Bouche PS, Delzon S, Choat B, Badel E, Brodrribb TJ, Burlett R, Cochard H, Charra - Vaskou K,**
 357 **Lavigne B, Li S** (2015) Are needles of *Pinus pinaster* more vulnerable to xylem embolism than
 358 branches? New insights from X - ray computed tomography. *Plant, cell & environment*
- 359 **Brodersen CR, McElrone AJ, Choat B, Lee EF, Shackel KA, Matthews MA** (2013) In vivo visualizations
 360 of drought-induced embolism spread in *Vitis vinifera*. *Plant physiology* **161**: 1820-1829
- 361 **Brodrribb TJ, Bienaimé D, Marmottant P** (2016) Revealing catastrophic failure of leaf networks under
 362 stress. *Proceedings of the National Academy of Sciences* **113**: 4865-4869
- 363 **Brodrribb TJ, Bowman DJMS, Nichols S, Delzon S, Burlett R** (2010) Xylem function and growth rate
 364 interact to determine recovery rates after exposure to extreme water deficit. *New*
 365 *Phytologist* **188**: 533-542
- 366 **Brodrribb TJ, Cochard H** (2009) Hydraulic Failure Defines the Recovery and Point of Death in Water-
 367 Stressed Conifers. *Plant Physiology* **149**: 575-584
- 368 **Brodrribb TJ, Holbrook NM** (2003) Stomatal closure during leaf dehydration, correlation with other
 369 leaf physiological traits. *Plant Physiology* **132**: 2166-2173
- 370 **Brodrribb TJ, McAdam SA, Jordan GJ, Martins SC** (2014) Conifer species adapt to low-rainfall climates
 371 by following one of two divergent pathways. *Proceedings of the National Academy of*
 372 *Sciences* **111**: 14489-14493
- 373 **Brodrribb TJ, Skelton RP, McAdam SA, Bienaimé D, Lucani CJ, Marmottant P** (2016) Visual
 374 quantification of embolism reveals leaf vulnerability to hydraulic failure. *New Phytologist*
 375 **209**: 1403-1409
- 376 **Charrier G, Torres-Ruiz JM, Badel E, Burlett R, Choat B, Cochard H, Delmas CE, Domec J-C, Jansen S,**
 377 **King A** (2016) Evidence for hydraulic vulnerability segmentation and lack of xylem refilling
 378 under tension. *Plant physiology*: pp. 01079.02016
- 379 **Choat B, Badel E, Burlett R, Delzon S, Cochard H, Jansen S** (2015) Non-invasive measurement of
 380 vulnerability to drought induced embolism by X-ray microtomography. *Plant Physiology* **170**:
 381 273-282
- 382 **Choat B, Brodersen CR, McElrone AJ** (2015) Synchrotron X-ray microtomography of xylem embolism
 383 in *Sequoia sempervirens* saplings during cycles of drought and recovery. *New Phytologist*
 384 **205**: 1095-1105
- 385 **Cochard H** (2002) A technique for measuring xylem hydraulic conductance under high negative
 386 pressures. *Plant Cell and Environment* **25**: 815-819
- 387 **Cochard H, Badel E, Herbette S, Delzon S, Choat B, Jansen S** (2013) Methods for measuring plant
 388 vulnerability to cavitation: a critical review. *Journal of Experimental Botany* **64**: 4779-4791
- 389 **Cochard H, Damour G, Bodet C, Tharwat I, Poirier M, Ameglio T** (2005) Evaluation of a new
 390 centrifuge technique for rapid generation of xylem vulnerability curves. *Physiologia*
 391 *Plantarum* **124**: 410-418
- 392 **Cochard H, Delzon S** (2013) Hydraulic failure and repair are not routine in trees. *Annals of Forest*
 393 *Science* **70**: 659-661
- 394 **Cuneo IF, Knipfer T, Brodersen CR, McElrone AJ** (2016) Mechanical failure of fine root cortical cells
 395 initiates plant hydraulic decline during drought. *Plant physiology* **172**: 1669-1678
- 396 **Delzon S, Douthe C, Sala A, Cochard H** (2010) Mechanism of water - stress induced cavitation in
 397 conifers: bordered pit structure and function support the hypothesis of seal capillary -
 398 seeding. *Plant, Cell & Environment* **33**: 2101-2111

399 **Ennajeh M, Simões F, Khemira H, Cochard H** (2011) How reliable is the double-ended pressure
400 sleeve technique for assessing xylem vulnerability to cavitation in woody angiosperms?
401 *Physiologia Plantarum* **142**: 205-210

402 **Hacke UG, Venturas MD, MacKinnon ED, Jacobsen AL, Sperry JS, Pratt RB** (2015) The standard
403 centrifuge method accurately measures vulnerability curves of long - vesselled olive stems.
404 *New Phytologist* **205**: 116-127

405 **Haines F** (1935) Observations on the occurrence of air in conducting tracts. *Annals of Botany*: 367-
406 379

407 **Hochberg U, Windt CW, Ponomarenko A, Zhang Y-J, Gersony J, Rockwell FE, Holbrook NM** (2017)
408 Stomatal closure, basal leaf embolism and shedding protect the hydraulic integrity of grape
409 stems. *Plant Physiology*

410 **Lamy J-B, Bouffier L, Burlett R, Plomion C, Cochard H, Delzon S** (2011) Uniform selection as a
411 primary force reducing population genetic differentiation of cavitation resistance across a
412 species range. *PLoS One* **6**: e23476

413 **Larter M, Pfautsch S, Domec J-C, Trueba S, Nagalingum N, Delzon S** Aridity drove the evolution of
414 extreme embolism resistance and the radiation of conifer genus *Callitris*. *New Phytologist*:
415 n/a-n/a

416 **Markesteyn L, Poorter L, Paz H, Sack L, Bongers F** (2011) Ecological differentiation in xylem
417 cavitation resistance is associated with stem and leaf structural traits. *Plant Cell and*
418 *Environment* **34**: 137-148

419 **Nolf M, Lopez R, Peters JMR, Flavel RJ, Koladin LS, Young IM, Choat B** (2017) Visualization of
420 xylem embolism by X-ray microtomography: a direct test against hydraulic measurements.
421 *New Phytologist* **214**: 890-898

422 **Pammenter N, Van der Willigen C** (1998) A mathematical and statistical analysis of the curves
423 illustrating vulnerability of xylem to cavitation. *Tree Physiology* **18**: 589-593

424 **Ponomarenko A, Vincent O, Pietriga A, Cochard H, Badel É, Marmottant P** (2014) Ultrasonic
425 emissions reveal individual cavitation bubbles in water-stressed wood. *Journal of The Royal*
426 *Society Interface* **11**: 20140480

427 **Rockwell FE, Wheeler JK, Holbrook NM** (2014) Cavitation and Its Discontents: Opportunities for
428 Resolving Current Controversies. *Plant physiology* **164**: 1649-1660

429 **Scoffoni C, Albuquerque C, Brodersen CR, Townes SV, John GP, Cochard H, Buckley TN, McElrone**
430 **AJ, Sack L** (2017) Leaf vein xylem conduit diameter influences susceptibility to embolism and
431 hydraulic decline. *New Phytologist* **213**: 1076-1092

432 **Skelton RP, Brodribb TJ, Choat B** (2017) Casting light on xylem vulnerability in an herbaceous species
433 reveals a lack of segmentation. *New Phytologist*

434 **Sperry JS, Hacke UG, Pittermann J** (2006) Size and function in conifer tracheids and angiosperm
435 vessels. *American Journal of Botany* **93**: 1490-1500

436 **Torres - Ruiz JM, Cochard H, Mayr S, Beikircher B, Diaz - Espejo A, Rodriguez - Dominguez CM,**
437 **Badel E, Fernández JE** (2014) Vulnerability to cavitation in *Olea europaea* current - year
438 shoots: further evidence of an open - vessel artifact associated with centrifuge and air -
439 injection techniques. *Physiologia Plantarum* **152**: 465-474

440 **Torres Ruiz JM, Cochard H, Mencuccini M, Delzon S, Badel E** (2016) Direct observation and
441 modelling of embolism spread between xylem conduits: a case study in Scots pine. *Plant, cell*
442 *& environment* **39**: 2774-2785

443 **Tyree M, Cochard H, Cruiziat P, Sinclair B, Ameglio T** (1993) Drought - induced leaf shedding in
444 walnut: evidence for vulnerability segmentation. *Plant, Cell & Environment* **16**: 879-882

445 **Urli M, Porté AJ, Cochard H, Guengant Y, Burlett R, Delzon S** (2013) Xylem embolism threshold for
446 catastrophic hydraulic failure in angiosperm trees. *Tree physiology* **33**: 672-683

447 **Vesque J** (1883) Observation directe du mouvement de l'eau dans les vaisseaux des plantes. *Annals*
448 *de Science Naturelles Botanique* **15**: 5-15

- 449 **Vinya R, Malhi Y, Fisher JB, Brown N, Brodribb TJ, Aragao LE** (2013) Xylem cavitation vulnerability
450 influences tree species' habitat preferences in miombo woodlands. *Oecologia* **173**: 711-720
451 **Xu X, Medvigy D, Powers JS, Becknell JM, Guan K** (2016) Diversity in plant hydraulic traits explains
452 seasonal and inter-annual variations of vegetation dynamics in seasonally dry tropical forests.
453 *New Phytologist* **212**: 80-95
454 **Zhang F-P, Brodribb TJ** (2017) Are flowers vulnerable to xylem cavitation during drought? *In Proc. R.*
455 *Soc. B*, Vol 284. The Royal Society, p 20162642
456 **Zimmermann MH** (1983) *Xylem Structure and the Ascent of Sap*. Springer-Verlag, Berlin
457

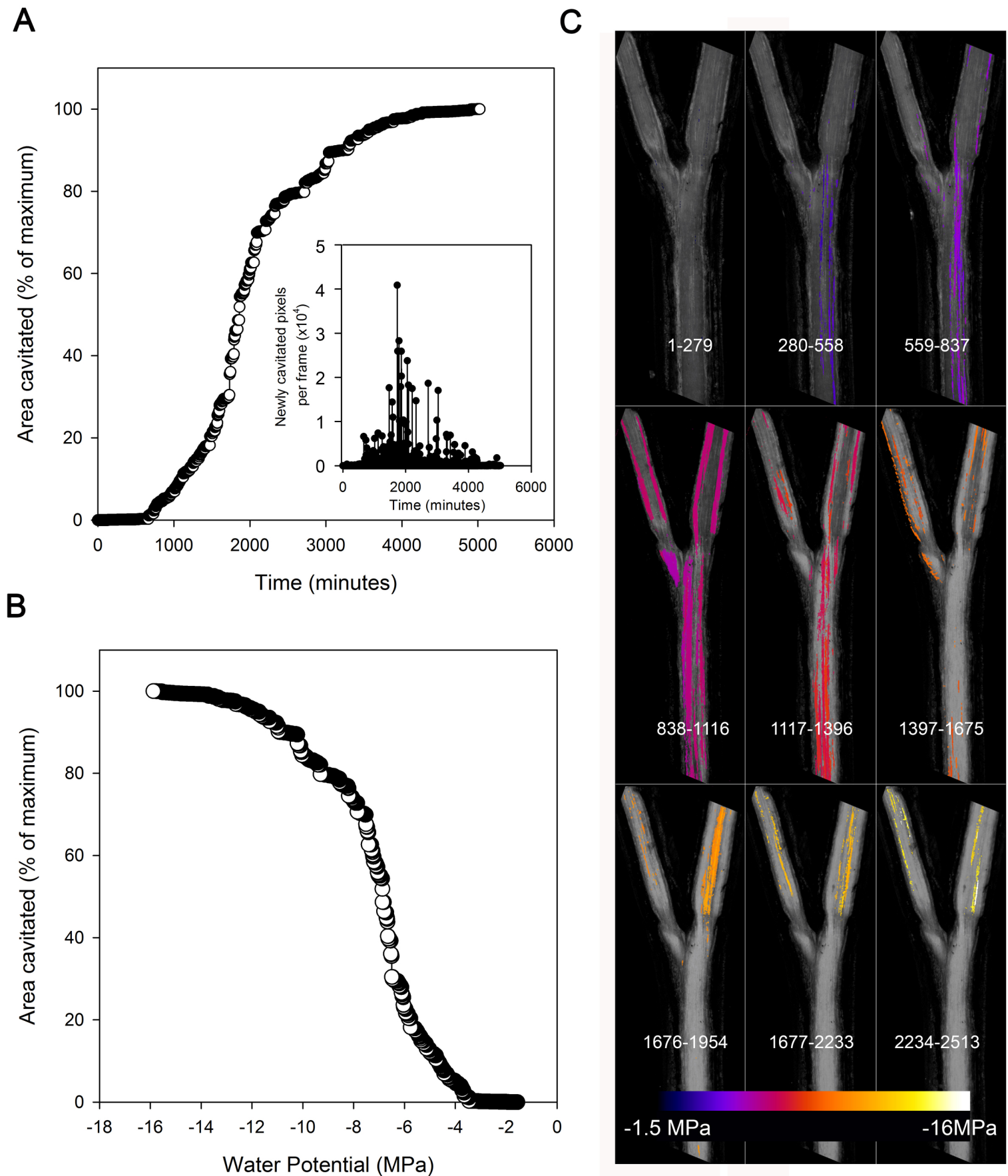


Figure 1. A- Cumulative area of cavitated xylem in a sample stem of *Callitris rhomboidea* is shown to increase rapidly approximately 1 day after a hydrated branch was excised (time zero) and allowed to dry. After a rapid rise in cavitation the rate of new xylem cavitated (quantified as number of pixels) falls back to zero approximately 3 days after excision. The insert graph shows that the size of newly cavitated regions visualized in the stem reaches a maximum during the steepest part of the curve (insert). During this period, very large blocks of tracheids were cavitating in the 2 minute interval between scans. B- Cumulative area of cavitated xylem expressed as a function of stem water potential showing a classic sigmoidal vulnerability curve. C- A mosaic of colour maps showing the spatial progression of cavitation through time in this 20mm long branched sample, the same stem sample as B and C. Sequential blocks of 280 images have been stacked together (frame numbers shown at the lower portion of each tile), with cavitated pixels coloured according to the water potential at which cavitation occurred. In this sample the smaller branches proved to be more resistant to cavitation than the main branch.

Downloaded from on August 16, 2017 - Published by www.plantphysiol.org
Copyright © 2017 American Society of Plant Biologists. All rights reserved.

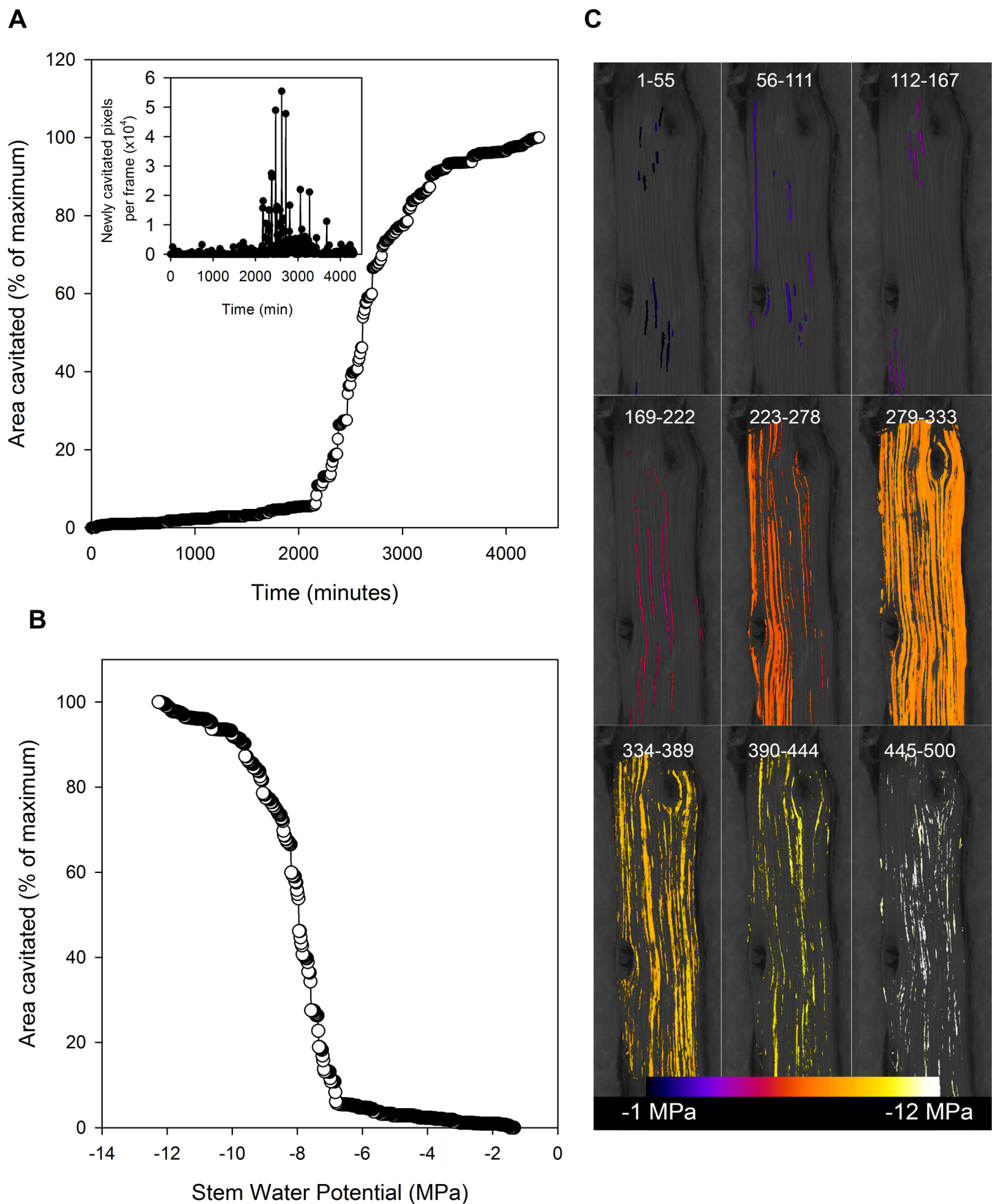


Figure 2. Similar plots as in Fig.1 showing the progression of cavitation in a stem of the angiosperm *Rosmarinus officinalis*. Despite the extreme resistance to cavitation in this stem the vulnerability curve shows a very steep transition from 12 to 88% cavitation. The reason for this steep transition can be clearly seen as due to a number of large and long cavitations between frames 279 and 333.

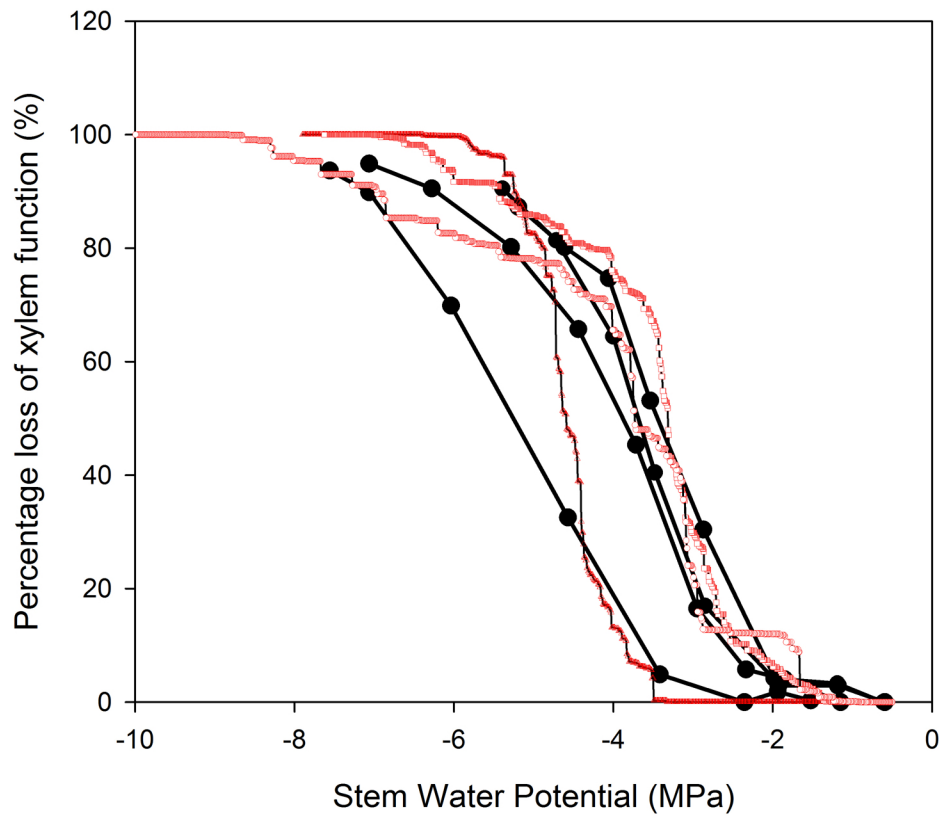


Figure 3. A comparison of vulnerability curve shape produced by the cavitron (black circles) and the optical method using branches from the same three individuals of the conifer *Lagarostrobos franklinii*. Although the mean P50 is very similar in both species, the slope of the curves between 12% and 88% were steeper using the optical method.

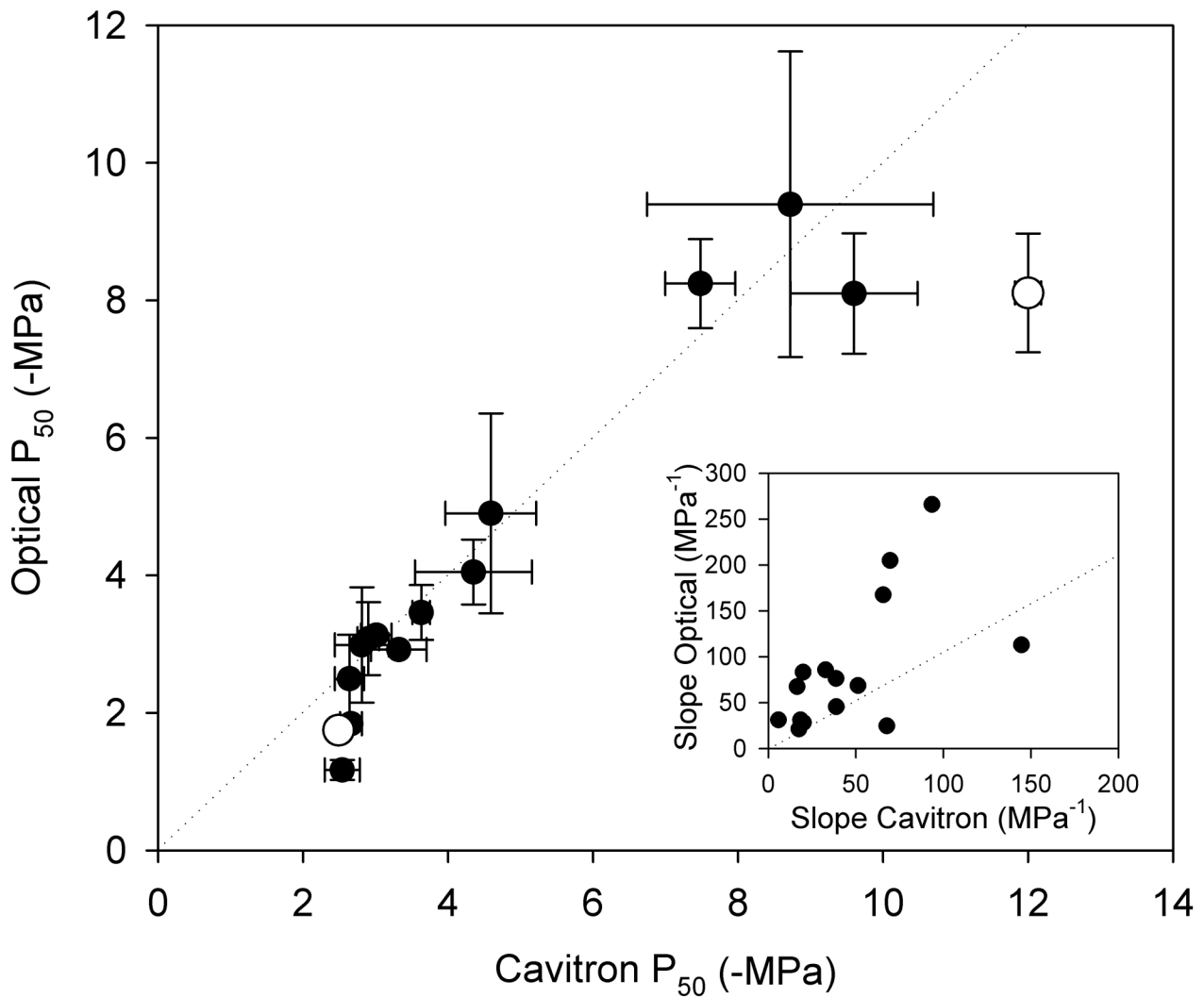


Figure 4. Mean P₅₀ (\pm sd) for stems of the same individuals measured with the optical and cavitron methods. Very close agreement was found in the conifer sample between methods (regression slope 0.98; $r^2=0.93$). Among the two angiosperms sampled, good agreement was found in one species, while the cavitron method produced a more negative P₅₀ in the second. Slopes produced by the two techniques (insert graph) were correlated ($r^2=0.35$; $p<0.05$), but the optical technique produced a steeper slope in 14/16 species (1:1 shown as dotted line in each plot).

Parsed Citations

Anderegg WRL, Flint A, Huang C-y, Flint L, Berry JA, Davis FW, Sperry JS, Field CB (2015) Tree mortality predicted from drought-induced vascular damage. *Nature Geosci* 8: 367-371

Pubmed: [Author and Title](#)

CrossRef: [Author and Title](#)

Google Scholar: [Author Only](#) [Title Only](#) [Author and Title](#)

Blackman CJ, Brodribb TJ, Jordan GJ (2012) Leaf hydraulic vulnerability influences species' bioclimatic limits in a diverse group of woody angiosperms. *Oecologia* 168: 1-10

Pubmed: [Author and Title](#)

CrossRef: [Author and Title](#)

Google Scholar: [Author Only](#) [Title Only](#) [Author and Title](#)

Bouche PS, Delzon S, Choat B, Badel E, Brodribb TJ, Burtlett R, Cochard H, Charra-Vaskou K, Lavigne B, Li S (2015) Are needles of *Pinus pinaster* more vulnerable to xylem embolism than branches? New insights from X-ray computed tomography. *Plant, cell & environment*

Pubmed: [Author and Title](#)

CrossRef: [Author and Title](#)

Google Scholar: [Author Only](#) [Title Only](#) [Author and Title](#)

Brodersen CR, McElrone AJ, Choat B, Lee EF, Shackel KA, Matthews MA (2013) In vivo visualizations of drought-induced embolism spread in *Vitis vinifera*. *Plant physiology* 161: 1820-1829

Pubmed: [Author and Title](#)

CrossRef: [Author and Title](#)

Google Scholar: [Author Only](#) [Title Only](#) [Author and Title](#)

Brodribb TJ, Bienaimé D, Marmottant P (2016) Revealing catastrophic failure of leaf networks under stress. *Proceedings of the National Academy of Sciences* 113: 4865-4869

Pubmed: [Author and Title](#)

CrossRef: [Author and Title](#)

Google Scholar: [Author Only](#) [Title Only](#) [Author and Title](#)

Brodribb TJ, Bowman DJMS, Nichols S, Delzon S, Burtlett R (2010) Xylem function and growth rate interact to determine recovery rates after exposure to extreme water deficit. *New Phytologist* 188: 533-542

Pubmed: [Author and Title](#)

CrossRef: [Author and Title](#)

Google Scholar: [Author Only](#) [Title Only](#) [Author and Title](#)

Brodribb TJ, Cochard H (2009) Hydraulic Failure Defines the Recovery and Point of Death in Water-Stressed Conifers. *Plant Physiology* 149: 575-584

Pubmed: [Author and Title](#)

CrossRef: [Author and Title](#)

Google Scholar: [Author Only](#) [Title Only](#) [Author and Title](#)

Brodribb TJ, Holbrook NM (2003) Stomatal closure during leaf dehydration, correlation with other leaf physiological traits. *Plant Physiology* 132: 2166-2173

Pubmed: [Author and Title](#)

CrossRef: [Author and Title](#)

Google Scholar: [Author Only](#) [Title Only](#) [Author and Title](#)

Brodribb TJ, McAdam SA, Jordan GJ, Martins SC (2014) Conifer species adapt to low-rainfall climates by following one of two divergent pathways. *Proceedings of the National Academy of Sciences* 111: 14489-14493

Pubmed: [Author and Title](#)

CrossRef: [Author and Title](#)

Google Scholar: [Author Only](#) [Title Only](#) [Author and Title](#)

Brodribb TJ, Skelton RP, McAdam SA, Bienaimé D, Lucani CJ, Marmottant P (2016) Visual quantification of embolism reveals leaf vulnerability to hydraulic failure. *New Phytologist* 209: 1403-1409

Pubmed: [Author and Title](#)

CrossRef: [Author and Title](#)

Google Scholar: [Author Only](#) [Title Only](#) [Author and Title](#)

Charrier G, Torres-Ruiz JM, Badel E, Burtlett R, Choat B, Cochard H, Delmas CE, Domec J-C, Jansen S, King A (2016) Evidence for hydraulic vulnerability segmentation and lack of xylem refilling under tension. *Plant physiology*: pp. 01079.02016

Pubmed: [Author and Title](#)

CrossRef: [Author and Title](#)

Google Scholar: [Author Only](#) [Title Only](#) [Author and Title](#)

Choat B, Badel E, Burtlett R, Delzon S, Cochard H, Jansen S (2015) Non-invasive measurement of vulnerability to drought induced embolism by X-ray microtomography. *Plant Physiology* 170: 273-282

Pubmed: [Author and Title](#)

CrossRef: [Author and Title](#)

Google Scholar: [Author Only](#) [Title Only](#) [Author and Title](#)

Choat B, Brodersen CR, McElrone AJ (2015) Synchrotron X-ray microtomography of xylem embolism in *Sequoia sempervirens* saplings during cycles of drought and recovery. *New Phytologist* 205: 1095-1105

Pubmed: [Author and Title](#)

CrossRef: [Author and Title](#)

Google Scholar: [Author Only](#) [Title Only](#) [Author and Title](#)

Cochard H (2002) A technique for measuring xylem hydraulic conductance under high negative pressures. *Plant Cell and Environment* 25: 815-819

Pubmed: [Author and Title](#)

CrossRef: [Author and Title](#)

Google Scholar: [Author Only](#) [Title Only](#) [Author and Title](#)

Cochard H, Badel E, Herbette S, Delzon S, Choat B, Jansen S (2013) Methods for measuring plant vulnerability to cavitation: a critical review. *Journal of Experimental Botany* 64: 4779-4791

Pubmed: [Author and Title](#)

CrossRef: [Author and Title](#)

Google Scholar: [Author Only](#) [Title Only](#) [Author and Title](#)

Cochard H, Damour G, Bodet C, Tharwat I, Poirier M, Ameglio T (2005) Evaluation of a new centrifuge technique for rapid generation of xylem vulnerability curves. *Physiologia Plantarum* 124: 410-418

Pubmed: [Author and Title](#)

CrossRef: [Author and Title](#)

Google Scholar: [Author Only](#) [Title Only](#) [Author and Title](#)

Cochard H, Delzon S (2013) Hydraulic failure and repair are not routine in trees. *Annals of Forest Science* 70: 659-661

Pubmed: [Author and Title](#)

CrossRef: [Author and Title](#)

Google Scholar: [Author Only](#) [Title Only](#) [Author and Title](#)

Cuneo IF, Knipfer T, Brodersen CR, McElrone AJ (2016) Mechanical failure of fine root cortical cells initiates plant hydraulic decline during drought. *Plant physiology* 172: 1669-1678

Pubmed: [Author and Title](#)

CrossRef: [Author and Title](#)

Google Scholar: [Author Only](#) [Title Only](#) [Author and Title](#)

Delzon S, Douthe C, Sala A, Cochard H (2010) Mechanism of water-stress induced cavitation in conifers: bordered pit structure and function support the hypothesis of seal capillary-seeding. *Plant, Cell & Environment* 33: 2101-2111

Pubmed: [Author and Title](#)

CrossRef: [Author and Title](#)

Google Scholar: [Author Only](#) [Title Only](#) [Author and Title](#)

Ennajeh M, Simões F, Khemira H, Cochard H (2011) How reliable is the double-ended pressure sleeve technique for assessing xylem vulnerability to cavitation in woody angiosperms? *Physiologia Plantarum* 142: 205-210

Pubmed: [Author and Title](#)

CrossRef: [Author and Title](#)

Google Scholar: [Author Only](#) [Title Only](#) [Author and Title](#)

Hacke UG, Venturas MD, MacKinnon ED, Jacobsen AL, Sperry JS, Pratt RB (2015) The standard centrifuge method accurately measures vulnerability curves of long-vesselled olive stems. *New Phytologist* 205: 116-127

Pubmed: [Author and Title](#)

CrossRef: [Author and Title](#)

Google Scholar: [Author Only](#) [Title Only](#) [Author and Title](#)

Haines F (1935) Observations on the occurrence of air in conducting tracts. *Annals of Botany*: 367-379

Pubmed: [Author and Title](#)

CrossRef: [Author and Title](#)

Google Scholar: [Author Only](#) [Title Only](#) [Author and Title](#)

Hochberg U, Windt CW, Ponomarenko A, Zhang Y-J, Gersony J, Rockwell FE, Holbrook NM (2017) Stomatal closure, basal leaf embolism and shedding protect the hydraulic integrity of grape stems. *Plant Physiology*

Pubmed: [Author and Title](#)

CrossRef: [Author and Title](#)

Google Scholar: [Author Only](#) [Title Only](#) [Author and Title](#)

Lamy J-B, Bouffier L, Burrett R, Plomion C, Cochard H, Delzon S (2011) Uniform selection as a primary force reducing population genetic differentiation of cavitation resistance across a species range. *PLoS One* 6: e23476

Pubmed: [Author and Title](#)

CrossRef: [Author and Title](#)

Google Scholar: [Author Only](#) [Title Only](#) [Author and Title](#)

Larter M, Pfautsch S, Domec J-C, Trueba S, Nagalingum N, Delzon S Aridity drove the evolution of extreme embolism resistance and the radiation of conifer genus *Callitris*. *New Phytologist*: n/a-n/a

Markestijn L, Poorter L, Paz H, Sack L, Bongers F (2011) Ecological differentiation in xylem cavitation resistance is associated with stem and leaf structural traits. *Plant Cell and Environment* 34: 137-148

Pubmed: [Author and Title](#)

CrossRef: [Author and Title](#)

Google Scholar: [Author Only](#) [Title Only](#) [Author and Title](#)

Nolf M, Lopez R, Peters JMR, Flavel RJ, Koloadin LS, Young IM, Choat B (2017) Visualization of xylem embolism by X-ray microtomography: a direct test against hydraulic measurements. *New Phytologist* 214: 890-898

Pubmed: [Author and Title](#)

CrossRef: [Author and Title](#)

Google Scholar: [Author Only](#) [Title Only](#) [Author and Title](#)

- Pammerter N, Van der Willigen C (1998) A mathematical and statistical analysis of the curves illustrating vulnerability of xylem to cavitation. *Tree Physiology* 18: 589-593**
Pubmed: [Author and Title](#)
CrossRef: [Author and Title](#)
Google Scholar: [Author Only](#) [Title Only](#) [Author and Title](#)
- Ponomarenko A, Vincent O, Pietriga A, Cochard H, Badel É, Marmottant P (2014) Ultrasonic emissions reveal individual cavitation bubbles in water-stressed wood. *Journal of The Royal Society Interface* 11: 20140480**
Pubmed: [Author and Title](#)
CrossRef: [Author and Title](#)
Google Scholar: [Author Only](#) [Title Only](#) [Author and Title](#)
- Rockwell FE, Wheeler JK, Holbrook NM (2014) Cavitation and Its Discontents: Opportunities for Resolving Current Controversies. *Plant physiology* 164: 1649-1660**
Pubmed: [Author and Title](#)
CrossRef: [Author and Title](#)
Google Scholar: [Author Only](#) [Title Only](#) [Author and Title](#)
- Scoffoni C, Albuquerque C, Brodersen CR, Townes SV, John GP, Cochard H, Buckley TN, McElrone AJ, Sack L (2017) Leaf vein xylem conduit diameter influences susceptibility to embolism and hydraulic decline. *New Phytologist* 213: 1076-1092**
Pubmed: [Author and Title](#)
CrossRef: [Author and Title](#)
Google Scholar: [Author Only](#) [Title Only](#) [Author and Title](#)
- Skelton RP, Brodribb TJ, Choat B (2017) Casting light on xylem vulnerability in an herbaceous species reveals a lack of segmentation. *New Phytologist***
Pubmed: [Author and Title](#)
CrossRef: [Author and Title](#)
Google Scholar: [Author Only](#) [Title Only](#) [Author and Title](#)
- Sperry JS, Hacke UG, Pittermann J (2006) Size and function in conifer tracheids and angiosperm vessels. *American Journal of Botany* 93: 1490-1500**
Pubmed: [Author and Title](#)
CrossRef: [Author and Title](#)
Google Scholar: [Author Only](#) [Title Only](#) [Author and Title](#)
- Torres-Ruiz JM, Cochard H, Mayr S, Beikircher B, Diaz-Espejo A, Rodriguez-Dominguez CM, Badel E, Fernández JE (2014) Vulnerability to cavitation in *Olea europaea* current-year shoots: further evidence of an open-vessel artifact associated with centrifuge and air-injection techniques. *Physiologia Plantarum* 152: 465-474**
Pubmed: [Author and Title](#)
CrossRef: [Author and Title](#)
Google Scholar: [Author Only](#) [Title Only](#) [Author and Title](#)
- Torres Ruiz JM, Cochard H, Mencuccini M, Delzon S, Badel E (2016) Direct observation and modelling of embolism spread between xylem conduits: a case study in Scots pine. *Plant, cell & environment* 39: 2774-2785**
Pubmed: [Author and Title](#)
CrossRef: [Author and Title](#)
Google Scholar: [Author Only](#) [Title Only](#) [Author and Title](#)
- Tyree M, Cochard H, Cruiziat P, Sinclair B, Ameglio T (1993) Drought-induced leaf shedding in walnut: evidence for vulnerability segmentation. *Plant, Cell & Environment* 16: 879-882**
Pubmed: [Author and Title](#)
CrossRef: [Author and Title](#)
Google Scholar: [Author Only](#) [Title Only](#) [Author and Title](#)
- Urli M, Porté AJ, Cochard H, Guengant Y, Burlett R, Delzon S (2013) Xylem embolism threshold for catastrophic hydraulic failure in angiosperm trees. *Tree physiology* 33: 672-683**
Pubmed: [Author and Title](#)
CrossRef: [Author and Title](#)
Google Scholar: [Author Only](#) [Title Only](#) [Author and Title](#)
- Vesque J (1883) Observation directe du mouvement de l'eau dans les vaisseaux des plantes. *Annals de Science Naturelles Botanique* 15: 5-15**
Pubmed: [Author and Title](#)
CrossRef: [Author and Title](#)
Google Scholar: [Author Only](#) [Title Only](#) [Author and Title](#)
- Vinya R, Malhi Y, Fisher JB, Brown N, Brodribb TJ, Aragao LE (2013) Xylem cavitation vulnerability influences tree species' habitat preferences in miombo woodlands. *Oecologia* 173: 711-720**
Pubmed: [Author and Title](#)
CrossRef: [Author and Title](#)
Google Scholar: [Author Only](#) [Title Only](#) [Author and Title](#)
- Xu X, Medvigy D, Powers JS, Becknell JM, Guan K (2016) Diversity in plant hydraulic traits explains seasonal and inter-annual variations of vegetation dynamics in seasonally dry tropical forests. *New Phytologist* 212: 80-95**
Pubmed: [Author and Title](#)
CrossRef: [Author and Title](#)
Google Scholar: [Author Only](#) [Title Only](#) [Author and Title](#)
- Zhang F-P, Brodribb TJ (2017) Are flowers vulnerable to xylem cavitation during drought? In *Proc. R. Soc. B, Vol 284. The Royal Society***

Society, p 20162642

Pubmed: [Author and Title](#)

CrossRef: [Author and Title](#)

Google Scholar: [Author Only](#) [Title Only](#) [Author and Title](#)

Zimmermann MH (1983) Xylem Structure and the Ascent of Sap. Springer-Verlag, Berlin

Pubmed: [Author and Title](#)

CrossRef: [Author and Title](#)

Google Scholar: [Author Only](#) [Title Only](#) [Author and Title](#)